

Lepton Flavour Violation in a radiative neutrino mass model with the asymmetric Yukawa structure

Yoko Irie^a, Osamu Seto^{b,c}, Tetsuo Shindou^d

^a*Department of Applied Physics,
Kogakuin University, Hachioji, Tokyo, 192-0015, Japan*

^b*Institute for the Advancement of Higher Education,
Hokkaido University, Sapporo 060-0817, Japan*

^c*Department of Physics,
Hokkaido University, Sapporo 060-0810, Japan*

^d*Division of Liberal-arts,
Kogakuin University, Hachioji, Tokyo, 192-0015, Japan*

Abstract

Though models with the radiative neutrino mass generation are phenomenologically attractive, the complicated relationship between the flavour structure of additional Yukawa matrices and the neutrino mass matrix sometimes is a barrier to explore the models. We introduce a simple prescription to analyze the relation in a class of models with the asymmetric Yukawa structure. We then apply the treatment to the Zee-Babu model as a concrete example of the class and discuss the phenomenological consequences of the model. The combined studies among the neutrino physics, the lepton flavour violation, and the search for the new particles at the collider experiments provide the anatomy of the Zee-Babu model.

1. Introduction

The neutrino oscillation experiments show that neutrinos have finite masses. The masses are several orders of magnitude smaller than the electron mass so that the origin of neutrino masses seems to be different from the other Standard Model (SM) fermions whose masses are generated through the Yukawa couplings with the Higgs boson. It is a big mystery in the SM what is the origin of such tiny neutrino masses.

There are many attractive ideas to address the origin of the neutrino mass. The most popular one is the canonical seesaw mechanism [1–5] where heavy sterile neutrinos are introduced into the SM, and the dimension-five operator so-called the Weinberg operator [6] is induced after the integration of the heavy sterile neutrinos. The coefficient of the Weinberg operator is suppressed by the very large mass scale of the sterile neutrinos, which is usually taken to be larger than 10^6 GeV. There are another class of models in which the tininess of the neutrino mass is responsible for the tiny vacuum expectation value (VEV) of an extra scalar field. A popular realisation of this idea is the type-II seesaw

model [7–12] where a $SU(2)$ triplet scalar field develops its tiny VEV. If the neutrino Yukawa coupling with the extra scalar field is of the order of 0.1, the VEV of the extra scalar field is expected to be as small as 1 eV.

An alternative approach to the origin of neutrino masses is that the tiny neutrino masses are generated through the quantum loop effect. Since the first model of this class was proposed by A. Zee [13], many interesting models have been proposed. A comprehensive review of this class of models can be found, for example, in Ref. [14]. Such models are phenomenologically attractive because the new particles are introduced at around the TeV scale or below. A model can be explored through a new particle direct production by future collider experiments as well as significant contributions to the flavour physics by new particles.

Since the neutrino oscillation parameters become precisely determined by the experiments [15], the Lagrangian parameters such as Yukawa coupling matrices with the extra scalars are restricted to reproduce the correct neutrino mass matrix. However, in many models, the relation between the Lagrangian parameters and the parameters in the induced neutrino mass matrix is not simple. The neutrino mass matrix is given by a product of several matrices, including relevant Yukawa coupling matrices, and there are additional degrees of freedom that cannot be determined by the input of the neutrino parameters. This will be a barrier to explore the models by flavour phenomenology.

Nevertheless, as far as models with loop generated neutrino masses are concerned, a comprehensive classification of the models based on the flavour structure has been completed in Refs. [16, 17]. The models which induce Majorana neutrino masses are classified into only three groups, and the models with Dirac neutrino masses are classified into seven groups. This is a great step to a systematic analysis of the phenomenological feature of the models.

In this article, we focus on a group of the models with the asymmetric Yukawa structure, to which the Zee-Babu model [18, 19] and the Krauss-Nasri-Trodden model [20] belong as popular examples. We propose a convenient treatment of relations between the Lagrangian parameters and the neutrino mass matrix. Once we find the treatment, it is easy to apply it to a concrete model and to study flavour phenomenology.

We will then demonstrate how our treatment works in the Zee-Babu model as an example. In the Zee-Babu model, a singly charged singlet scalar and a doubly charged singlet scalar are contained, and the neutrino masses are induced at the two-loop. Rich phenomenology in the model has been widely studied in the literature, for instance, see Refs. [21–26]. Utilizing the relation between the Lagrangian parameters and the neutrino mass matrix, we can systematically analyze the flavour phenomenology in the model, and we will show the constraint on the CP phases in the neutrino mixing matrix.

This letter is organized as follows. In Sec. 2, we show how to extract the Yukawa matrices in the Lagrangian by the input of the neutrino mass matrix. In Sec. 3, we apply the treatment to the Zee-Babu model, and we analyze the phenomenological feature of the Zee-Babu model. We give Summary in Sec. 4.

2. Flavour structure

Though there are many models with radiative Majorana neutrino mass generation proposed, those can be classified into only three groups by their flavour structure [16]. We here focus on models of the Group-I in Ref [16], in which the light neutrino mass matrix M_ν is given by

$$M_\nu \propto Y_\omega m_\ell X_S m_\ell Y_\omega^T \equiv M, \quad (1)$$

where Y_ω is an anti-symmetric matrix, X_S is a symmetric matrix, and $m_\ell \equiv \text{diag}(m_e, m_\mu, m_\tau)$ is a diagonal matrix with charged lepton masses. In general, this class of models contains a new singlet singly charged scalar ω^\pm , which can have flavour anti-symmetric Yukawa interactions with lepton doublets as

$$\mathcal{L} = \frac{1}{2} (Y_\omega)^{ij} \epsilon_{ab} \bar{\ell}_{Li}^c \ell_{Lj}^b \omega^+ + \text{h.c.}, \quad (2)$$

where ℓ_{Li} denotes the left-handed SM lepton doublet field, $i, j = e, \mu, \tau$ are flavour indexes, the superscript c denotes the charge conjugation and $a, b = 1, 2$ are SU(2) indexes. Note that we take the basis that the charged leptons are mass eigenstates. The origin of the symmetric matrix X_S depends on the detail of each model.

One can write the neutrino mass matrix M_ν in terms of the neutrino observables as

$$M_\nu = U^* \begin{pmatrix} m_1 & 0 & 0 \\ 0 & m_2 & 0 \\ 0 & 0 & m_3 \end{pmatrix} U^\dagger, \quad (3)$$

where $m_{1,2,3}$ are the mass eigenvalues of the light neutrinos and U is the Pontecorvo-Maki-Nakagawa-Sakata (PMNS) matrix[27, 28]. The PMNS matrix U is parameterized as

$$U = \begin{pmatrix} c_{12}c_{13} & s_{12}c_{13} & s_{13}e^{-i\delta} \\ -s_{12}c_{23} - c_{12}s_{13}s_{23}e^{i\delta} & c_{12}c_{23} - s_{12}s_{13}s_{23}e^{i\delta} & c_{13}s_{23} \\ s_{12}s_{23} - c_{12}s_{13}c_{23}e^{i\delta} & -c_{12}s_{23} - s_{12}s_{13}c_{23}e^{i\delta} & c_{13}c_{23} \end{pmatrix} \begin{pmatrix} e^{i\eta_1} & 0 & 0 \\ 0 & e^{i\eta_2} & 0 \\ 0 & 0 & 1 \end{pmatrix}, \quad (4)$$

with the abbreviations $c_{ij} = \cos \theta_{ij}$ and $s_{ij} = \sin \theta_{ij}$, and δ being the Dirac CP phase. Eq. (1) provides $\det(M_\nu) = 0$, which means that the lightest neutrino is massless so that either m_1 or m_3 is zero. Because of this, the Majorana phase η_1 can always be eliminated by the phase redefinition of the neutrino fields, and we set $\eta_1 = 0$ in the following. The cases with $m_1 = 0$ and $m_3 = 0$ correspond to the normal ordering (NO) and the inverted ordering (IO) neutrino masses. Tab. 1 shows the values of the neutrino parameters obtained from the global analysis of the current neutrino data.

Table 1: The values of the neutrino parameters obtained from the global analysis. The numbers are taken from Ref. [15] (the analysis without the Super-Kamiokande atmospheric data).

	Normal Ordering		Inverted Ordering	
	Best Fit	3 σ range	Best Fit	3 σ range
$\theta_{12}/^\circ$	33.44	31.27 – 35.86	33.45	31.27 – 35.87
$\theta_{23}/^\circ$	49.0	39.6 – 51.8	49.3	39.9 – 52.0
$\theta_{13}/^\circ$	8.57	8.20 – 8.97	8.61	8.24 – 8.98
$\delta/^\circ$	195	107 – 403	286	192 – 360
$\Delta m_{21}^2/10^{-5} \text{ eV}^2$	7.42	6.82 – 8.04	7.42	6.82 – 8.04
$\Delta m_{3\ell}^2/10^{-3} \text{ eV}^2$	2.514	2.431–2.598	–2.497	–2.583 – –2.412

To explore the property of the flavour structure in Eq. (1), we parameterise Y_ω and X_S as

$$Y_\omega = \begin{pmatrix} 0 & f_{12} & f_{13} \\ -f_{12} & 0 & f_{23} \\ -f_{13} & -f_{23} & 0 \end{pmatrix}, \quad X_S = \begin{pmatrix} X_{11} & X_{12} & X_{13} \\ X_{12} & X_{22} & X_{23} \\ X_{13} & X_{23} & X_{33} \end{pmatrix}. \quad (5)$$

Since $m_e \ll m_\mu \ll m_\tau$ is satisfied, we can neglect the terms with m_e in M so that the elements $X_{1i} (i = 1, 2, 3)$ become irrelevant to the neutrino mass matrix. This approximation leads to

$$M = Y_\omega m_\ell X_S m_\ell Y_\omega^T = \begin{pmatrix} * & * & * \\ * & m_\tau^2 f_{23}^2 X_{33} & -m_\mu m_\tau f_{23}^2 X_{23} \\ * & -m_\mu m_\tau f_{23}^2 X_{23} & m_\mu^2 f_{23}^2 X_{22} \end{pmatrix}. \quad (6)$$

for the right lower 2×2 part of M . Within the 3σ parameter range given in Tab. 1, $|M_{22}| \sim |M_{23}| \sim |M_{33}| \sim \mathcal{O}(0.01) \text{ eV}$ is satisfied in most area of the allowed parameter space for both the NO and the IO masses¹. Therefore, it is reasonable to parameterise X_{22} and X_{33} as

$$X_{33} = \alpha \frac{m_\mu}{m_\tau} X_{23}, \quad X_{22} = \beta \frac{m_\tau}{m_\mu} X_{23}, \quad (7)$$

with two complex parameters α and β whose absolute values are of the order of one. By introducing k and k' as

$$f_{12} = k f_{23}, \quad f_{13} = k' f_{23}, \quad (8)$$

we can write the neutrino mass matrix as

$$M_\nu \propto M = X_{23} f_{23}^2 m_\mu m_\tau \begin{pmatrix} \beta k^2 + 2kk' + \alpha k'^2 & k + \alpha k' & -\beta k - k' \\ k + \alpha k' & \alpha & -1 \\ -\beta k - k' & -1 & \beta \end{pmatrix}, \quad (9)$$

¹In certain points of the IO case, either M_{22} or M_{33} becomes tiny.

which leads to

$$\alpha = -\frac{(M_\nu)_{22}}{(M_\nu)_{23}}, \quad \beta = -\frac{(M_\nu)_{33}}{(M_\nu)_{23}}, \quad (10)$$

$$k = \frac{1}{\alpha\beta - 1} \left(\frac{(M_\nu)_{12}}{(M_\nu)_{23}} + \alpha \frac{(M_\nu)_{13}}{(M_\nu)_{23}} \right), \quad k' = -\frac{1}{\alpha\beta - 1} \left(\beta \frac{(M_\nu)_{12}}{(M_\nu)_{23}} + \frac{(M_\nu)_{13}}{(M_\nu)_{23}} \right). \quad (11)$$

Therefore, all the relevant parameters besides the overall factor $X_{22}f_{23}^2$ are determined by the neutrino parameters. Since the experimental 3σ range of δ is still wide, and there is no restriction on η_1 and η_2 , the parameters α , β , k , and k' vary in a certain range shown in Tab. 2.

Table 2: The allowed range of the parameters α , β , k , and k' , when the neutrino parameters are scanned in the 3σ range given in Tab. 1.

	Normal Ordering	Inverted Ordering
$ \alpha $	$0.57 \leq \alpha \leq 1.6$	$0.0 \leq \alpha \leq 2.4$
$\arg(\alpha)$	$-\pi \leq \arg(\alpha) \leq \pi$	$-\pi \leq \arg(\alpha) \leq \pi$
$ \beta $	$0.52 \leq \beta \leq 1.6$	$0.0 \leq \beta \leq 2.8$
$\arg(\beta)$	$-\pi \leq \arg(\beta) \leq \pi$	$-\pi \leq \arg(\beta) \leq \pi$
$ k $	$0.27 \leq k \leq 0.67$	$3.9 \leq k \leq 5.3$
$\arg(k)$	$-0.27 \leq \arg(k) \leq 0.32$	$-2.9 \leq \arg(k) \leq 0$
$ k' $	$0.26 \leq k' \leq 0.66$	$4.0 \leq k' \leq 5.4$
$\arg(k')$	$-0.33 \leq \arg(k') \leq 0.33$	$0.21 \leq \arg(k') \leq \pi$

In this class of models, the singlet singly charged particle contributes to lepton flavour violation processes such as $\mu \rightarrow e\gamma$ via loop diagrams shown in Fig. 1. When this contribution is dominant, the branching ratio of $\mu \rightarrow e\gamma$ is proportional to $|f_{13}^*f_{23}|^2 = |k'|^2|f_{23}|^4$. It may imply an upper bound on $|k'|$. A concrete example of the constraint from this issue is shown in the next section.

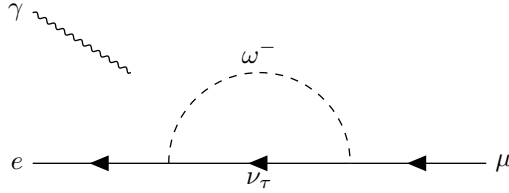


Figure 1: One loop diagram with ω contributing to $\mu \rightarrow e\gamma$ at the one-loop level.

3. Lepton flavour violation in the Zee-Babu model

The Zee-Babu model [18, 19] is a famous concrete example of the class of models discussed in the previous section. In this model, a singlet doubly charged scalar κ^{--} is introduced in addition to ω^- . The relevant part of the Lagrangian is given by

$$\mathcal{L}_{\text{ZB}} = - \sum_{i,j=1}^3 (Y_\omega)^{ij} \bar{\ell}_{Li}^c \cdot \ell_{Lj} \omega^+ - \sum_{i,j=1}^3 (Y_\kappa)^{ij} \bar{e}_{Ri}^{[e]} e_{Rj}^c \kappa^{--} - \mu_{\text{ZB}} \omega^- \omega^- \kappa^{++} + \text{h.c.} . \quad (12)$$

The neutrino mass matrix is generated at the two-loop level through the diagram shown in Fig. 2. Each element of the induced neutrino mass matrix is given by

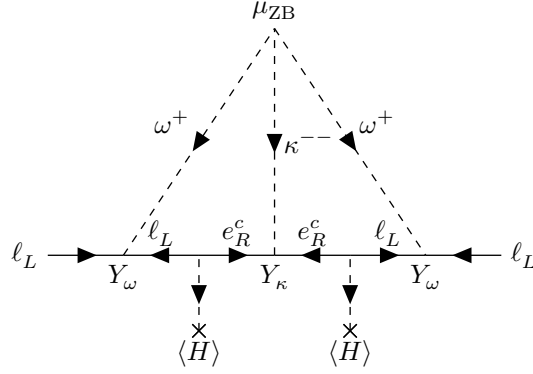


Figure 2: The diagram relevant to the neutrino mass matrix in the Zee-Babu model.

$$(M_\nu)^{ij} = \left(\frac{1}{16\pi^2} \right)^2 \sum_{k,l=1}^3 \frac{16\mu_{\text{ZB}}}{M_\kappa^2} (Y_\omega)^{ik} m_{e_k} (Y_\kappa)^{kl} m_{e_l} (Y_\omega)^{jl} I(M_\omega^2, 0 | M_\omega^2, 0 | M_\kappa^2) , \quad (13)$$

where M_ω^2 and M_κ^2 are the physical mass eigenvalues of the extra scalars, ω^- and κ^{--} . The loop function $I(m_{11}^2, m_{12}^2 | m_{12}^2, m_{22}^2 | M^2)$ is given by [29, 30],

$$I(m_{11}^2, m_{12}^2 | m_{12}^2, m_{22}^2 | M^2) = \frac{1}{\pi^4} \int d^4 p \int d^4 q \frac{M^2}{(p^2 + m_{11}^2)(p^2 + m_{12}^2)(q^2 + m_{21}^2)(q^2 + m_{22}^2)((p+q)^2 + M^2)} . \quad (14)$$

In the approximation with $m_{e_i} = 0$, the loop function can be evaluated as [21, 22],

$$I(M_\omega^2, 0|M_\omega^2, 0|M_\kappa^2) = - \int_0^1 dx \int_0^{1-x} dy \frac{r}{x + (r-1)y + y^2} \log \frac{y(1-y)}{x+ry} \\ \simeq \begin{cases} 2.8r^2(r+0.31)^{-1.5}, & (r \gtrsim 1), \\ 1.98r(r+0.12)^{-0.23}, & (r < 1), \end{cases} \quad (15)$$

where $r = M_\kappa^2/M_\omega^2$. The symmetric matrix X_S in Eq. (1) can be identified with the Yukawa coupling matrix, Y_κ . Therefore, the relevant part of Y_κ and Y_ω can be parameterized in the way shown in the previous section.

In the Zee-Babu model, there are mainly two types of contributions to the LFV processes. One is the singlet doubly charged scalar exchange at the tree level, which causes the LFV three body decays as $e_i^- \rightarrow e_j^- e_k^- e_l^+$. The decay width is given by

$$\Gamma(e_i^- \rightarrow e_j^- e_k^- e_l^+) = \frac{C_{jk}}{8} \frac{m_{e_i}^5}{192\pi^3} \left| \frac{(Y_\kappa)^{il}(Y_\kappa)^{*jk}}{M_\kappa^2} \right|^2, \quad (16)$$

where C_{jk} denotes a statistical factor as

$$C_{jk} = \begin{cases} 1 & (j = k) \\ 2 & (j \neq k) \end{cases}. \quad (17)$$

Another is a one-loop contribution to $e_i \rightarrow e_j \gamma$ via the same type of the diagram shown in Fig. 1. The decay width of $e_i \rightarrow e_j \gamma$ is given by

$$\Gamma(e_i \rightarrow e_j + \gamma) = \frac{\alpha_e}{4} m_{e_i}^5 \left(|A_L^{ji}|^2 + |A_R^{ji}|^2 \right), \quad (18)$$

with $\alpha_e = e^2/(4\pi)$ and

$$A_L^{ji} \simeq - \frac{1}{(4\pi)^2} \frac{(Y_\omega)^{*kj}(Y_\omega)^{ki}}{3M_\omega^2}, \quad A_R^{ji} = - \frac{1}{(4\pi)^2} \frac{4(Y_\kappa)^{*kj}(Y_\kappa)^{ki}}{3M_\kappa^2}. \quad (19)$$

As discussed in the previous section, the elements $(Y_\kappa)_{i1}$ are irrelevant to the neutrino mass matrix. In the following, we fix $(Y_\kappa)_{i1} = 0$ for simplicity. If non-zero $(Y_\kappa)_{i1}$ is taken into account, $\text{Br}(\mu \rightarrow e\gamma)$ becomes enhanced.

Let us first consider the NO neutrino case. In this case, $(Y_\kappa)_{22} \neq 0$ is satisfied within the 3σ range of neutrino parameters listed in Tab. 1. Once the neutrino parameters m_i , θ_{ij} , δ , η_1 , and η_2 , and massive parameters M_ω , M_κ , and μ_{ZB} are fixed, the element $(M_\nu)_{23}$ determines the size of $f_{23}^2 Y_{23}$. It leads to a strong correlation $\text{Br}(\mu \rightarrow e\gamma)^2 \propto \text{Br}(\tau \rightarrow \mu\mu\mu)$. This correlation is displayed in Fig. 3. One can see that $\text{Br}(\mu \rightarrow e\gamma)$ is minimized when $\text{Br}(\tau \rightarrow \mu\mu\mu)$ is maximized as $\text{Br}(\tau \rightarrow \mu\mu\mu) = 2.1 \times 10^{-8}$ which is the upper limit from the experiment [31].

In Fig. 4, we show the dependence of the minimal value of $\text{Br}(\mu \rightarrow e\gamma)$ on the Dirac CP phase in the PMNS matrix, δ . The other oscillation parameters are

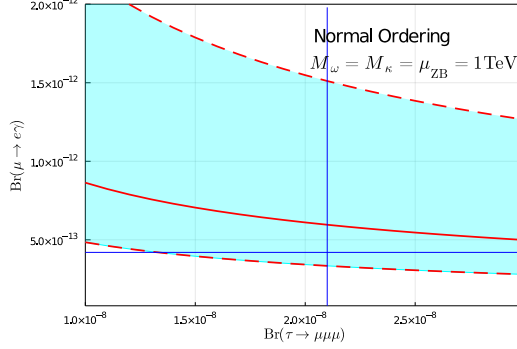


Figure 3: The correlation between $\text{Br}(\tau \rightarrow \mu\mu\mu)$ and the minimal value of $\text{Br}(\mu \rightarrow e\gamma)$ in the NO case is shown. The massive model parameters are fixed as $M_\omega = M_\kappa = \mu_{\text{ZB}} = 1.0 \text{ TeV}$. The shaded region is obtained by scanning the other oscillation parameters in the 3σ range shown in Tab. 1 and scanning η_2 in $0 \leq \eta_2 \leq 2\pi$. On the solid red curve, the neutrino oscillation parameters are fixed to be the best fit values listed in Tab. 1 and $\eta_2 = 0$. The horizontal and vertical blue solid lines show the current upper bound on $\text{Br}(\mu \rightarrow e\gamma)$ and $\text{Br}(\tau \rightarrow \mu\mu\mu)$.

scanned in the 3σ range given in Tab. 1, the Majorana CP phase η_2 is scanned in the range $0 \leq \eta_2 \leq 2\pi$, and we fix the massive parameters in the extra scalar sector as $M_\omega = M_\kappa = \mu_{\text{ZB}} = 1.0 \text{ TeV}$. We take the maximal value of $|Y_{23}|$ which leads to $\text{Br}(\tau \rightarrow \mu\mu\mu) = 2.1 \times 10^{-8}$, in order to minimize $|f_{23}|$ and $\text{Br}(\mu \rightarrow e\gamma)$.

Fig. 5 shows the contour of $\text{Br}(\mu \rightarrow e\gamma)$ on the parameter plane of η_2 and δ . The other neutrino parameters are scanned within the 3σ range. The solid red curves correspond to the current upper bound $\text{Br}(\mu \rightarrow e\gamma) = 4.2 \times 10^{-13}$ [32], and the area between these two curves is the allowed region.

In Fig. 6, we show the contour of the minimal value of $\text{Br}(\mu \rightarrow e\gamma)$ in each point on the parameter plane of a extra scalar mass M_ω or M_κ and μ_{ZB} . The LHC bound on the extra scalar masses is studied in the literature [24–26], and the region of $m_\kappa, m_\omega > 500 \text{ GeV}$ is not constrained by the direct search of extra particles. The neutrino parameters are scanned within the 3σ range given in Tab. 1, and η_2 is considered in $-\pi \leq \eta_2 \leq \pi$. In the figures (a), (b), and (c), we consider the case with $M_\omega = M_\kappa$, $M_\omega = 10M_\kappa$, and $M_\kappa = 10M_\omega$, respectively. The left-below area of the solid red curve in each figure is excluded by the current experimental bound of $\text{Br}(\mu \rightarrow e\gamma)$. Since the $\text{Br}(\mu \rightarrow e\gamma)$ is dominated by the ω exchange diagram, the constraint is significantly relaxed for $M_\omega \gg M_\kappa$ case. On the other hand, the contribution to $\text{Br}(\tau \rightarrow \mu\mu\mu)$ is suppressed in $M_\kappa \gg M_\omega$, and the size of $|f_{23}|$ can be small. Therefore, the constraint is relaxed in comparison to the $M_\omega = M_\kappa$ case. Let us comment on the case with large μ_{ZB} . If μ_{ZB} is too large compared to M_ω and M_κ , the electroweak vacuum might be unstable, so that such a case might be constrained. The quantitative study of vacuum stability is out of the scope of this paper. The sensitivity to $\text{Br}(\mu \rightarrow e\gamma)$ will go down to 6×10^{-14} at the MEG-II experiment [33], and a

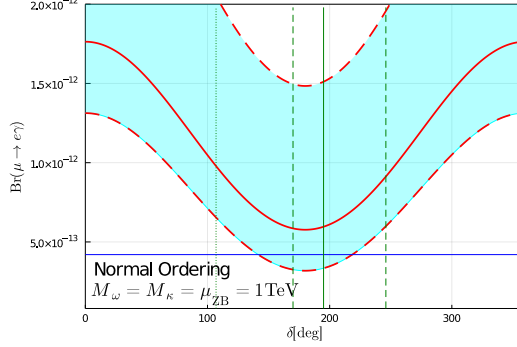


Figure 4: The dependence of the minimal value of $\text{Br}(\mu \rightarrow e\gamma)$ on the Dirac CP phase in the PMNS matrix, δ . $M_\omega = M_\kappa = \mu_{\text{ZB}} = 1.0$ TeV. The shaded region is obtained by scanning the other oscillation parameters except for δ in the 3σ range shown in Tab. 1 and scanning η_2 in $0 \leq \eta_2 \leq 2\pi$. On the red solid curve, the neutrino oscillation parameters are fixed to be the best fit values listed in Tab. 1 and $\eta_2 = 0$. The $(Y_\kappa)_{23}$ is determined to satisfy $\text{Br}(\tau \rightarrow \mu\mu\mu) = 2.1 \times 10^{-8}$. The horizontal solid line shows the upper bound on $\text{Br}(\mu \rightarrow e\gamma)$. The vertical solid line denotes the best fit value of δ . The dashed and dotted line are the boundary of the 1σ and 3σ allowed range of δ , respectively.

wider region of the parameter space will be explored.

In the IO case, $(Y_\kappa)_{22} = 0$ is realized in a certain set of the neutrino mixing parameters. In such parameter points, $\text{Br}(\tau \rightarrow \mu\mu\mu)$ satisfies the experimental limit with the rather large value of $(Y_\kappa)_{23}$ which makes f_{23} small enough to satisfy $\text{Br}(\mu \rightarrow e\gamma) < 4.3 \times 10^{-13}$. In Fig. 7, we show the contour plots of $\text{Br}(\tau \rightarrow \mu\mu\mu)$ on the plane of η_2 and δ , and on the plane of $\langle m \rangle$ and δ . Here, $\langle m \rangle$ is the effective Majorana mass parameter of the neutrinoless double beta decay, which is defined by

$$\langle m \rangle = \left| \sum_{i=1,2,3} m_i U_{ei}^2 \right|. \quad (20)$$

We scanned the other neutrino parameters within the 3σ range given in Tab. 1, and we tune the $|f_{23}|$ to be $\text{Br}(\mu \rightarrow e\gamma) = 4.3 \times 10^{-13}$ which is the current upper limit. The red curves show the experimental bound of $\text{Br}(\tau \rightarrow \mu\mu\mu)$, and inside the curve is allowed. By the strong constraint on the lepton flavour violation, the lower value of $\langle m \rangle$ is preferred.

4. Summary

We have discussed the lepton flavour violating processes and their phenomenological consequences in a class of models with radiative neutrino mass generation. We focus on the models where the induced neutrino mass matrix has a specific structure given by $M_\nu \propto Y_\omega m_\ell X_S m_\ell Y_\omega^T$. We have utilized an

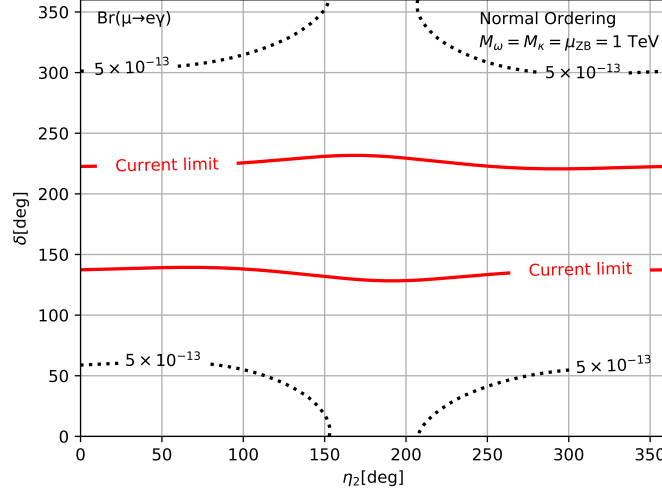


Figure 5: The contour of the minimal value of $\text{Br}(\mu \rightarrow e\gamma)$ on the η_2 - δ plane. The other neutrino oscillation parameters are scanned in the 3σ range shown in Tab. 1. We fix the massive parameters in the extra scalar sector as $M_\omega = M_\kappa = \mu_{\text{ZB}} = 1.0$ TeV. The solid curves corresponds to the current upper bound $\text{Br}(\mu \rightarrow e\gamma) = 4.2 \times 10^{-13}$.

approximation that the electron mass in m_ℓ is neglected, and we have found the relations between the neutrino mass matrix and the Yukawa coupling matrices of the extra scalars.

We have applied such relations to the Zee-Babu model as a concrete example. We have found that the lepton flavour violation processes, $\tau \rightarrow \mu\mu\mu$ and $\mu \rightarrow e\gamma$, are powerful tools to investigate the Zee-Babu model. They constrain the neutrino parameters as well as the massive parameters in the extra scalar sector.

The MEG-II will search $\mu \rightarrow e\gamma$ down to $\text{Br}(\mu \rightarrow e\gamma) \leq 6 \times 10^{-14}$ [33], and the expected sensitivity of the upper limit on $\text{Br}(\tau \rightarrow \mu\mu\mu)$ is 3.3×10^{-10} at the Belle-II experiment [34]. The neutrino parameters will be more precisely determined by the neutrino oscillation experiments. For example, if $\delta = 0$ or $\delta = 180^\circ$ is the case, the Dirac CP phase will be measured with the uncertainty of 7.2° at the Hyper-Kamiokande experiment [35]. The sensitivities of the other oscillation parameters will also be significantly improved.

In the near future, the Zee-Babu model can be probed by multiple searches for the lepton flavour violation, neutrino experiments, and new particle search at high energy collider experiments.

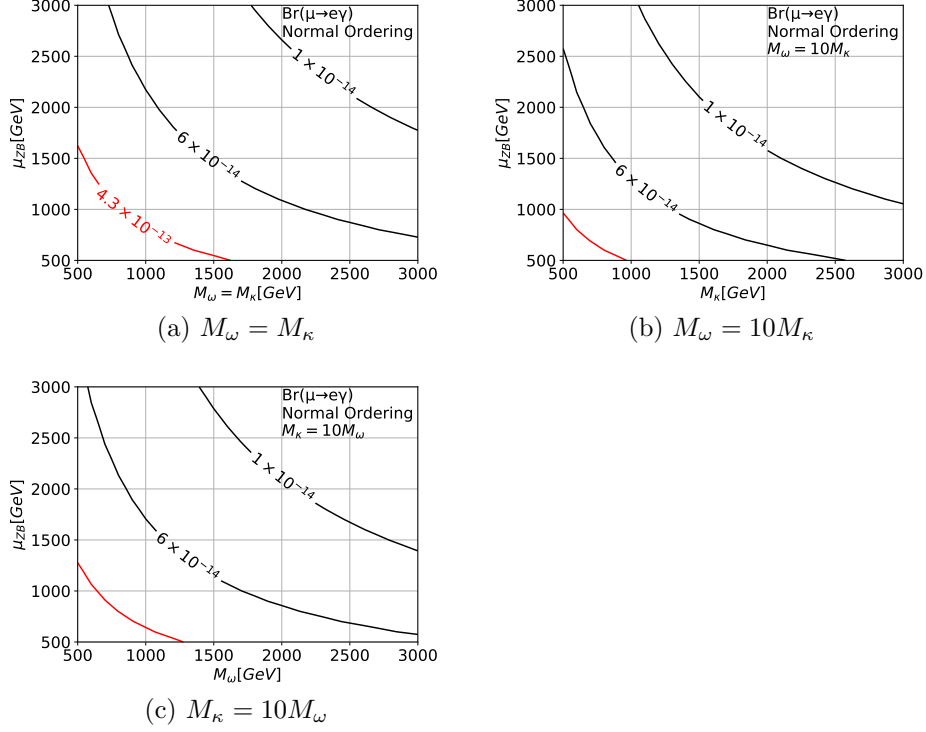


Figure 6: The contour of the minimal value of $\text{Br}(\mu \rightarrow e\gamma)$ in each point on the parameter plane of an extra scalar mass M_ω or M_κ and μ_{ZB} . Three patterns of the extra scalar masses are plotted as (a) $M_\omega = M_\kappa$, (b) $M_\omega = 10M_\kappa$, and (c) $M_\kappa = 10M_\omega$. The lower-left side of the red curve in each plot is excluded by the bound of $\text{Br}(\mu \rightarrow e\gamma)$. The neutrino parameters are scattered within the 3σ range given in Tab. 1, and the Majorana CP phase η_2 is considered in $-\pi \leq \eta_2 \leq \pi$.

Acknowledgments

This work is supported in part by the Japan Society for the Promotion of Science (JSPS) KAKENHI Grants No. 19K03860, No. 19K03865, No. 21H00060 (O.S.) and 20H00160 (T.S.).

References

- [1] P. Minkowski, Phys. Lett. 67B (1977) 421.
- [2] T. Yanagida, Conf. Proc. C 7902131 (1979) 95.
- [3] T. Yanagida, Prog.Theor.Phys. 64 (1980) 1103.

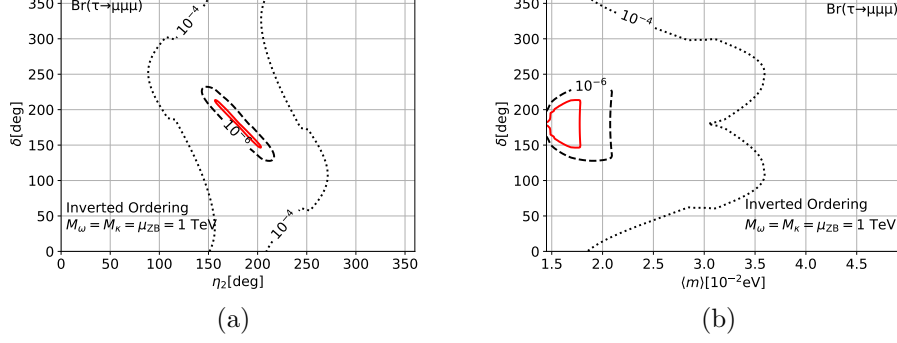


Figure 7: The contour of the minimal value of $\text{Tr}(\tau \rightarrow \mu\mu\mu)$ in the IO case are shown on (a) the η_2 - δ plane and (b) the $\langle m \rangle$ - δ plane. The other neutrino oscillation parameters are scanned in the 3σ range shown in Tab. 1. We fix the massive parameters in the extra scalar sector as $M_\omega = M_\kappa = \mu_{ZB} = 1.0$ TeV. The solid curves corresponds to the current upper bound $\text{Br}(\tau \rightarrow \mu\mu\mu) = 2.1 \times 10^{-8}$.

- [4] M. Gell-Mann, P. Ramond and R. Slansky, Conf.Proc. C790927 (1979) 315, 1306.4669.
- [5] R.N. Mohapatra and G. Senjanovic, Phys. Rev. Lett. 44 (1980) 912.
- [6] S. Weinberg, Phys. Rev. Lett. 43 (1979) 1566.
- [7] W. Konetschny and W. Kummer, Phys. Lett. B 70 (1977) 433.
- [8] T.P. Cheng and L.F. Li, Phys. Rev. D 22 (1980) 2860.
- [9] G. Lazarides, Q. Shafi and C. Wetterich, Nucl. Phys. B 181 (1981) 287.
- [10] J. Schechter and J.W.F. Valle, Phys. Rev. D 22 (1980) 2227.
- [11] M. Magg and C. Wetterich, Phys. Lett. B 94 (1980) 61.
- [12] R.N. Mohapatra and G. Senjanovic, Phys. Rev. D 23 (1981) 165.
- [13] A. Zee, Phys. Lett. 93B (1980) 389, [Erratum: Phys. Lett.95B,461(1980)].
- [14] Y. Cai et al., Front. in Phys. 5 (2017) 63, 1706.08524.
- [15] I. Esteban et al., JHEP 09 (2020) 178, 2007.14792.
- [16] S. Kanemura and H. Sugiyama, Phys. Lett. B 753 (2016) 161, 1510.08726.
- [17] S. Kanemura, K. Sakurai and H. Sugiyama, Phys. Lett. B 758 (2016) 465, 1603.08679.
- [18] A. Zee, Nucl. Phys. B 264 (1986) 99.

- [19] K.S. Babu, Phys. Lett. B 203 (1988) 132.
- [20] L.M. Krauss, S. Nasri and M. Trodden, Phys. Rev. D 67 (2003) 085002, hep-ph/0210389.
- [21] K.S. Babu and C. Macesanu, Phys. Rev. D 67 (2003) 073010, hep-ph/0212058.
- [22] D. Aristizabal Sierra and M. Hirsch, JHEP 12 (2006) 052, hep-ph/0609307.
- [23] M. Nebot et al., Phys. Rev. D 77 (2008) 093013, 0711.0483.
- [24] D. Schmidt, T. Schwetz and H. Zhang, Nucl. Phys. B 885 (2014) 524, 1402.2251.
- [25] J. Herrero-Garcia et al., Nucl. Phys. B 885 (2014) 542, 1402.4491.
- [26] J. Alcaide, M. Chala and A. Santamaria, Phys. Lett. B 779 (2018) 107, 1710.05885.
- [27] B. Pontecorvo, Zh. Eksp. Teor. Fiz. 34 (1957) 247.
- [28] Z. Maki, M. Nakagawa and S. Sakata, Prog. Theor. Phys. 28 (1962) 870.
- [29] J. van der Bij and M.J.G. Veltman, Nucl. Phys. B 231 (1984) 205.
- [30] K.L. McDonald and B.H.J. McKellar, (2003), hep-ph/0309270.
- [31] K. Hayasaka et al., Phys. Lett. B 687 (2010) 139, 1001.3221.
- [32] MEG, A.M. Baldini et al., Eur. Phys. J. C 76 (2016) 434, 1605.05081.
- [33] MEG II, A.M. Baldini et al., Eur. Phys. J. C 78 (2018) 380, 1801.04688.
- [34] Belle-II, W. Altmannshofer et al., PTEP 2019 (2019) 123C01, 1808.10567, [Erratum: PTEP 2020, 029201 (2020)].
- [35] Hyper-Kamiokande, K. Abe et al., (2018), 1805.04163.